

1 **Real-time optical analysis of a colorimetric LAMP assay for SARS-**
2 **CoV-2 in saliva with a handheld instrument improves accuracy**
3 **compared to endpoint assessment**

4

5 Running Title: SARS-CoV-2 colorimetric LAMP assay for saliva

6

7 Lena M. Diaz¹, Brandon E. Johnson², Daniel M. Jenkins^{1*}

8

9 Department of Molecular Biosciences and Bioengineering, College of Tropical Agriculture and

10 Human Resources, University of Hawaii at Manoa, Honolulu, HI, 96822, USA¹

11

12 Center for Biomedical Research, The Queen's Medical Center, Honolulu, HI, 96813, USA²

13

14

15 *Author for correspondence. Tel: (808) 781-1343; Fax: (808) 956-3542

16 E-mail: danielje@hawaii.edu

17

18

19

20

21 **Abstract**

22 Controlling the course of the COVID-19 pandemic will require widespread deployment
23 of consistent and accurate diagnostic testing of the novel coronavirus SARS-CoV-2. Ideally, tests
24 should detect a minimum viral load, be minimally invasive, and provide a rapid and simple
25 readout. Current FDA-approved RT-qPCR-based standard diagnostic approaches require
26 invasive nasopharyngeal swabs and involve laboratory-based analyses that can delay results.
27 Recently, a loop mediated isothermal nucleic acid amplification (LAMP) test that utilizes
28 colorimetric readout received FDA approval. This approach utilizes a pH indicator dye to detect
29 drop in pH from nucleotide hydrolysis during nucleic acid amplification. This method has only
30 been approved for use with RNA extracted from clinical specimens collected via nasopharyngeal
31 swabs. In this study, we developed a quantitative LAMP-based strategy to detect SARS-CoV-2
32 RNA in saliva. Our detection system distinguished positive from negative sample types using a
33 handheld instrument that monitors optical changes throughout the LAMP reaction. We used this
34 system in a streamlined LAMP testing protocol that could be completed in less than two hours to
35 directly detect inactivated SARS-CoV-2 in minimally processed saliva that bypassed RNA
36 extraction, with a limit of detection (LOD) of 50 genomes/reaction. The quantitative method
37 correctly detected virus in 100% of contrived clinical samples spiked with inactivated SARS-
38 CoV-2 at either 1X (50 genomes/reaction) or 2X (100 genomes/reaction) of the LOD.
39 Importantly the quantitative method was based on dynamic optical changes during the reaction
40 so was able to correctly classify samples that were misclassified by endpoint observation of
41 color.

42 Key Words: COVID-19, diagnostics, near patient, RNA detection, sample preparation, RT-
43 LAMP, Coronavirus

44 **Introduction**

45

46 Widespread deployment of rapid, accurate diagnostics is one of several key requirements
47 for blunting the COVID-19 pandemic. Ideal tests are minimally invasive, requiring little or no
48 sample preparation steps, and can be conducted on-site with a rapid and simple readout of a test
49 outcome. However, the standard diagnostic approach requires an RNA extraction step from a
50 nasopharyngeal (NP) swab and subsequent Reverse Transcription-quantitative Polymerase Chain
51 Reaction (RT-qPCR). The invasiveness of the collection procedure often causes patient
52 discomfort, reducing enthusiasm for regular retesting. Swab samples must then be stored in a
53 viral transport medium (VTM) to stabilize the virus until the sample can be analyzed, usually
54 after shipping to off-site laboratories. Furthermore, RNA extraction and RT-PCR analysis
55 require specialized equipment and clinical laboratory training that are not easily adaptable to
56 near-patient analysis. Finally, slow sample processing and nucleic acid amplification procedures
57 cannot be significantly streamlined to facilitate rapid detection.

58 Testing saliva for RNA of respiratory viruses like SARS-CoV-2 has been shown to have
59 high agreement in performance and sensitivity to approved RT-qPCR based tests of NP swab-
60 based molecular tests.¹⁻³ Isothermal analogs to PCR such as loop-mediated isothermal
61 amplification (LAMP) can be implemented with comparatively simple and low-power equipment
62 ⁴⁻⁶ and has proven to reliably amplify synthetic SARS-CoV-2 genomic RNA from samples with
63 as few as five copies of template molecules per reaction.⁷ LAMP specifically is commonly
64 observed to be more robust than equivalent qPCR assays to inhibitors in clinical samples, so that
65 accurate results can be obtained even with rudimentary sample preparation (i.e. just add sample
66 mixed with extraction buffer).⁸⁻¹⁰ Even so, as of December, 2020, less than 3% of all

67 commercially available diagnostics with regulatory approval used for SARS-CoV-2 detection in
68 the United States FDA, European Union and Asia utilize isothermal technology.¹¹

69 The colorimetric SARS-CoV-2 LAMP diagnostic assay developed by COLOR was one
70 of the first of these isothermal assays to receive Emergency Use Authorization (EUA) by the
71 FDA.¹² In this assay pyrophosphate hydrolyzed during a positive amplification event lowers the
72 pH of the reaction buffer containing phenol red indicator, resulting in an observable change in
73 color.¹³ This assay has proven to have a low false negative rate when used in conjunction with
74 purified gamma-irradiated virus and purified viral clinical samples.¹² While other FDA-EUA
75 approved isothermal based methods have received FDA approval when used for serum or
76 respiratory samples (i.e. nasopharyngeal swabs),¹⁴⁻¹⁶ approvals for direct detection in saliva have
77 lagged behind no matter the molecular basis of the test. While SARS-CoV-2 RNA is as stable in
78 saliva as it is in VTM,^{1,17} the effects of saliva on direct LAMP detection is poorly understood and
79 VTM can interfere with the colorimetric readout.¹⁸ For example, variations in pH and buffering
80 capacity of individual saliva samples can confound results of pH-dependent assays such as
81 colorimetric LAMP, especially if relying on visual classification of endpoint color.

82 To date, the use of a colorimetric LAMP assay with clinical saliva samples has not been
83 reported. Applications of isothermal amplification to detect SARS-CoV-2 have utilized
84 commercially available polymerase enzyme mixes that contain nucleotides, Tris pH buffer, and
85 Tween detergent. Additional studies have optimized amplification efficiency of genomic RNA
86 from whole-virus samples resuspended in water by supplementing commercial reaction mixes
87 with guanidinium chloride,¹⁹ Tris-EDTA (TE) and Tween-20.²⁰ Detection sensitivity of whole
88 virus has been further optimized by pre-incubating viral samples at 95°C to denature the viral
89 capsid before adding samples to a LAMP reaction mix.²¹⁻²³ Sample processing protocols have not

90 been optimized for the direct detection of SARS-CoV-2 from saliva. In this work we report a
91 streamlined approach for direct detection of SARS-CoV-2 RNA in contrived saliva samples,
92 including simple sample preparation steps and monitoring of reactions in a hand-held instrument
93 for dynamic detection of color changes.

94

95

96 **Materials and Methods**

97

98 **SARS-CoV-2 RNA standards and controls**

99

100 For the experiments in this study, contrived samples consisting of water, buffers or saliva
101 were spiked with either synthetic RNA (BEI Resources catalog no. NR-52358, Lot no.
102 70035241) or gamma-irradiated (BEI Resources catalog no. NR-52287, Lot no. 70033322)
103 SARS-CoV-2 virus. The reported starting genome copy number, designated throughout this
104 study as genome equivalents (ge), for the synthetic RNA and gamma-irradiated SARS-CoV-2
105 are 1.05×10^8 ge/mL and 1.7×10^9 ge/mL (pre-inactivation) respectively. The following reagent
106 was deposited by the Center for Disease Control and Prevention and obtained through BEI
107 Resources, NIAID, NIH: Quantitative Synthetic RNA from SARS-Related Coronavirus 2, NR-
108 52358, SARS-Related Coronavirus 2, Isolate USA-WA1/2020 and Gamma-Irradiated, NR-
109 52287. The synthetic RNA includes fragments from the ORF 1ab, Envelope (E) and
110 Nucleocapsid (N) regions. All virus stocks were aliquoted into 10 single use individual stocks
111 and stored at -80°C . Stocks were diluted to the appropriate concentration in RNase/DNase-free
112 water each day before experimentation.

113

114 **Quantitative analysis of colorimetric-luminance readout**

115

116 *Instrumentation*

117 For real-time monitoring and quantitative detection of colorimetric LAMP assays we
118 customized a handheld, battery-powered, fluorescence-based instrument with a heating block
119 accommodating a strip of 8 PCR tubes (BioRanger™, Diagenetix Inc., Honolulu, HI, USA; Fig.
120 1A). The instrument interfaces to a companion Android app to monitor changes in color of the
121 reaction mix. The modifications made to the device were removal of emission filters, and
122 attenuation of raw signal by a combination of placing a diffuser over the photodiode detectors
123 and electrically lowering their transimpedance gains. The resulting luminance signal (L) in
124 arbitrary units (a.u.) results from scattering and reflections of excitation light not absorbed by the
125 sample. Changes in the luminance in the dynamically monitored system correspond primarily to
126 changes in absorbance of light by the sample. For sample illumination we tested three different
127 color LEDs (Luxeon Rebel Color Line, Lumileds Ltd., San Jose, CA): blue (part number LXML-
128 PB01-0040); green (part number LXML-PM01-0100), and; amber (part number LXML-PL01-
129 0040). Preliminary experiments (Supplementary Fig. S0) indicated that the green LEDs resulted
130 in features in positive amplification curves that were identifiable earlier in the reactions than
131 curves from other colors, and which could also be used for more definitive reaction
132 classification. Based on these preliminary results we used green channel for monitoring reactions
133 reported in this study, using quantitative analysis of amplification curves as described below.
134 Calibration of the instrument was made with representative endpoint reactions with negative

135 standards (pink solution, nominally assigned 0 a.u) and positive standards (yellow solution,
136 nominally assigned 60000 a.u.).

137

138 *Processing Luminance Data*

139 For detailed analysis of experimental reactions described in this manuscript we used the
140 raw “luminance” data from files generated automatically in the BioRanger app. Unless otherwise
141 stated, all values were shifted to start at “zero” luminance by subtracting the initial (t = 0
142 minutes) raw luminance value from every raw value. These baseline corrected luminance values
143 (L) were smoothed using a 2nd order polynomial with a rolling average of 4 adjacent data points.
144 The maximum values of luminance derivatives (L’) for each assay were identified from
145 derivative data (identified using forward difference and smoothed again with a 2nd order
146 polynomial with 4 neighbors) using GraphPad Prism 9 (GraphPad Software, San Diego, CA,
147 USA).

148

149 **LAMP assays**

150

151 *Primers*

152 Two previously published LAMP primer sets (Supplementary Table S1) developed by
153 New England BioLabs,²⁴ targeting the envelope (E1) and nucleocapsid (N2) genes of the SAR-
154 CoV-2 viral genome (GenBank accession number MN908947), were tested individually and in
155 combination. For the final contrived clinical evaluation an internal control (IC) primer set that
156 amplifies human β -actin “housekeeping” gene (ACTB) was used to detect the presence of
157 inhibitors in saliva samples. Primers were synthesized commercially (Integrated DNA

158 Technologies / IDT, Coralville, Iowa) using standard desalting and resuspended in nuclease free
159 water. For each primer set an individual 10X primer stock was prepared so that adding 2.5 μL of
160 each stock to a LAMP reaction yielded the following final primer concentrations in both
161 fluorescent and colorimetric LAMP assays: 0.2 μM F3/B3, 1.6 μM FIP/BIP and 0.8 μM LB/LF.
162 For LAMP assays containing dual primer sets targeting both the E and N gene of SARS-CoV-2
163 genome, 2.5 μL of each 10X stock were added to each reaction mixture.

164

165 *Colorimetric LAMP Assay*

166 All colorimetric assays contained 12.5 μL WarmStart[®] RT-Colorimetric 2X Master Mix
167 (DNA & RNA, M1800, New England Biolabs, MA, USA), 2.5 μL primer mix (10X) stock of
168 each primer set used (E1, N2 or ACTB), either 2 μL or 5 μL of sample and appropriate volumes
169 of nuclease free water to make a total volume of 25 μL per reaction. After loading LAMP
170 reagents and test samples a drop ($\sim 20 \mu\text{L}$) of sterile mineral oil was added to each reaction tube
171 (excluding some of the negative controls in preliminary evaluation) and closed, followed by brief
172 centrifugation of the 8-assay tube strip.

173 For reactions containing guanidine hydrochloride (GuHCl molecular grade, J7582322,
174 ThermoFischer Scientific, Waltham, MA, USA), 1.25 μL of GuHCl stock (0.8 M) was
175 substituted for the equivalent volume of nuclease free water to achieve a final reaction
176 concentration of 40 mM GuHCl. Stock GuHCl solution was prepared in deionized water and
177 adjusted to pH 8.0 with 1 M KOH (90% reagent grade, 484016, Sigma Aldrich, St. Louis, MO,
178 USA) and filter sterilized (0.22 μM 13 mm Whatman filter, 99091302, MilliporeSigma, St.
179 Louis, MO, USA).

180 All real-time colorimetric assays were carried out in 0.2 mL reaction tubes (TempAssure,
181 Optical Caps, USA Scientific Inc., Orlando, FL, USA) in a modified 8-well isothermal amplifier
182 platform (BioRanger). Amplification progress was logged every 30 seconds for a maximum of
183 40 minutes. At the end of the assay the closed tube strip was briefly placed on ice and a
184 photograph was taken using a cell phone camera. The colorimetric master mix contains a phenol
185 red pH indicator used for visual detection of amplification and interpreted according to
186 manufacturers (NEB) protocols²⁵ as follows: negative reactions remain pink while successful
187 amplification results in yellow or yellow/orange color observable by naked eye.

188

189 *Fluorescent LAMP Assay*

190 Fluorescent LAMP assays were performed in parallel to most colorimetric assays under
191 the same experimental and assay conditions except fluorescent assays included 0.5 μ L
192 fluorescent dye (50X, E1700S, New England Biolabs). Assays were performed in either a) 0.2
193 mL reaction tubes (TempAssure, Optical Caps, USA Scientific Inc., Orlando, FL, USA) in an
194 *unmodified* 8-well isothermal amplifier platform (BioRanger™, Diagenetix Inc., Honolulu, HI,
195 USA) or b) 0.1 mL reaction tubes (TempAssure, Optical Caps, USA Scientific Inc., Orlando, FL,
196 USA) in a real-time PCR machine (Applied Biosciences StepOnePlus™). Both instruments were
197 programmed for isothermal incubation at 65°C for 31 minutes. Fluorescence values
198 corresponding to fluorescein were recorded every minute during the 31-minute reactions in the
199 StepOnePlus™ PCR machine, and every 30 seconds in the BioRanger isothermal amplifier. For
200 the BioRanger, threshold times (t_T) of positively classified reactions are reported as the time at
201 which the maximum rate of fluorescence increase occurs, to control for variations in reaction
202 intensity and fluorescence sensitivity between channels. For the StepOnePlus™ PCR machine,

203 the t_T was estimated as the time required for the fluorescence value to exceed a threshold value
204 equivalent to the pooled average plus three standard deviations of the fluorescence values
205 observed throughout the reactions of triplicate negative control reactions.^{26,27}

206

207 **Quantitative colorimetric-LAMP assay development**

208

209 *Controls and Standards*

210 For preliminary assay optimization and characterization, positive control (PC) standards
211 containing 5.25 – 5,250 ge/ 5 μ L were prepared daily by dissolving synthetic SARS-CoV-2 RNA
212 from frozen stock in nuclease free deionized water, whereas negative controls (NC) did not
213 contain target template RNA. For contrived clinical sample testing reactive controls (RC)
214 containing 5×10^3 ge/mL – 1.0×10^6 ge/mL in the primary sample were prepared by spiking
215 saliva with inactivated (gamma-irradiated) SARS-CoV-2 RNA and non-reactive control (NRC)
216 samples are saliva without added template.

217

218 *Reaction Condition Optimization*

219 Fluorescent LAMP assays performed on a StepOnePlus™ PCR machine was used to
220 evaluate the effect of adding GuHCl, compare sensitivity of different LAMP primers, and
221 determine optimal reaction temperature for detection of viral RNA in water standards. 5 μ L
222 samples of each PC and NC standard was added to a LAMP assay to achieve 0 – 5,250
223 ge/reaction with or without GuHCl and incubated for 31 minutes at either 65°C or 68°C. Primer
224 sets were evaluated individually and duplexed (E1 + N2) by adding equal volumes (1:1) of stock
225 primer mixes to a LAMP reaction. The Limit of Detection (LOD) for each set of assay and

226 processing conditions was determined as the lowest concentration where detection occurred in
227 3/3 replicates of PC reactions.

228

229 *Quantitative Classification of Results from Luminance Data*

230 To identify features in luminance curves that consistently differentiated positive and
231 negative colorimetric LAMP reactions, we considered simple quantitative metrics from
232 amplification data recorded on the modified BioRanger device assaying RNA standards in water.
233 The value of each metric for discriminating the binary populations was evaluated in a
234 commercial software (GraphPad Software, San Diego, CA, USA) using unpaired t-test assuming
235 equal variances.

236 Based on these preliminary results, Reactions were classified based on the value of the
237 peak luminance derivative L' (a.u./min.), as strong peaks are consistent with sigmoidal
238 amplification characteristic of qPCR or LAMP. Classification thresholds were empirically
239 derived from baseline measurements of controls standards without viral RNA. The threshold for
240 positive classification was determined as the value excluding at least 99.9% of negative controls
241 (for standards in water prepared with viral RNA) or non-reactive controls (for contrived clinical
242 samples in saliva) based on observed means and sample standard deviations using a one-tailed t-
243 statistic. The LOD for colorimetric assay in standards or contrived clinical samples in the
244 modified instrument was defined as the lowest concentration (ge/mL) where all replicates were
245 positively detected by this metric.

246

247

248 **Application of the quantitative colorimetric-LAMP assay for SARS-CoV-2 in** 249 **saliva**

250

251 *Saliva Collection*

252 Approximately 1-3 mL of saliva was collected from healthy individual volunteers in 15
253 mL conical tubes (352196, Falcon™, Thermo Fisher Scientific, Waltham, MA, USA). Donors
254 were asked to not eat or drink anything other than water before saliva was collected. Saliva
255 samples were collected fresh on the mornings of experimentation and stored at 4 °C until
256 processed. On the day of each experiment saliva samples were spiked with known quantities of
257 inactivated (gamma-irradiated) SARS-CoV-2 virus following protocols described in this section.

258

259 *Standardized Processing and Assay of Contrived Clinical Samples*

260 In the absence of known positive COVID-19 clinical samples, we followed the Federal
261 Food and Drug Administration's (FDA) guidance for molecular diagnostic development for
262 Emergency Use Authorization²⁸ and validated the sensitivity and accuracy of the colorimetric
263 LAMP assay using contrived clinical samples. Saliva collected from three healthy donors
264 presumed to be free of SARS-CoV-2 virus was pooled and spiked with inactivated gamma
265 irradiated SARS-CoV-2. Spiked saliva samples were heat inactivated in a dry bath at 95 °C for
266 30 minutes, allowed to cool to room temperature then stored on ice until downstream processing.
267 100 μ L of each treated 1 mL spiked sample was combined with an equal volume (1:1) of
268 stabilization buffer containing 1X TE (10 mM Tris, 0.1 mM EDTA, pH 8, IDT) and 1% Tween-
269 20 for a final sample concentration of 0.5X TE and 0.5% Tween-20. 2 μ L of each sample was
270 added directly to the colorimetric LAMP reaction mix for detection of the SARS-CoV-2 N-gene

271 using the N2 primer set only. Reactions were analyzed by real-time colorimetric LAMP (65°C,
272 40 minutes) on a BioRanger diagnostic platform modified to measure luminance of colorimetric
273 reactions.

274

275 **Validation in contrived clinical samples**

276

277 Ten individual saliva specimens were collected from healthy donors and evaluated for the
278 real-time quantitative SARS-CoV-2 colorimetric LAMP assay. One milliliter of each of the 10
279 specimens was spiked with gamma-irradiated SARS-CoV-2 to produce five contrived positive
280 clinical samples with a viral load at 1X the previously established LOD of 5×10^4 ge/mL
281 corresponding to 50 ge/reaction and five contrived positive samples at 2X the LOD (1×10^5
282 ge/mL) corresponding to 100 ge/reaction. Unadulterated volumes from each original specimen
283 were assayed identically to serve as a paired non-reactive sample for each contrived positive
284 clinical sample. The 20 samples (10 negative and 10 positive) were randomized and blinded and
285 processed through the entire standardized assay procedure.

286 For every saliva sample (n=20) an eight-assay diagnostic test panel was performed to
287 simultaneously test two replicates each of the test sample, internal control (IC), positive control
288 (PC) and negative control (NC). Saliva samples were tested for SARS-CoV-2 N-gene and human
289 β -actin (IC). Positive controls contained 2.1×10^6 ge/reaction of synthetic SARS-CoV-2 RNA
290 (BEI 52358) dissolved in deionized water, and deionized water no template negative controls
291 were both tested for the N-gene. Each reaction in the panel contained 2 μ L of sample, 40 mM of
292 GuHCl and standard colorimetric master mix and primer concentrations as previously described.
293 Assays were carried out and interpreted blind to the experimenter. The corresponding viral load

294 in each sample for analysis was revealed at the end of the experiment only after the samples had
295 been analyzed by quantitative colorimetric LAMP. The results of each diagnostic panel were
296 interpreted by the experimenter both visually following the manufacturers protocol and
297 quantitatively based on luminance signals for each individual LAMP assay.

298

299

300 **Results**

301

302 **Reaction conditions**

303

304 Fluorescent LAMP assays were used to evaluate optimal reaction conditions for assays
305 containing single and duplexed primer sets. The addition of 40 mM GuHCl to fluorescent LAMP
306 assays improved both the speed and sensitivity for the detection of synthetic RNA in spiked
307 water controls. Assays containing only the N2 primer set and guanidine hydrochloride performed
308 best overall in terms of sensitivity (~ 5.25 genome equivalents/reaction) and speed of detection
309 (mean $t_T = 19$ minutes, Supplementary Fig. 1). The differences in the speed of detection for
310 duplexed reactions were unremarkable; E1 primers are less sensitive than the N2 primers by
311 approximately an order of magnitude in any condition. E1-primed reactions were also more
312 temperature sensitive: incubation at 68°C inhibited LAMP reactions. Colorimetric assays were
313 run ten minutes longer than fluorescent assays for a total time of 40 minutes to compensate for
314 the relatively slow color change of the phenol red indicator that has been demonstrated to take
315 forty to fifty minutes to detect single copy numbers of SARS-CoV-2 genomes in previous

316 studies.^{29,30} All subsequent colorimetric assays were performed under optimal conditions: 40 mM
317 GuHCl and incubated at 65°C for 40 minutes.

318

319 **Visual and quantitative evaluation of assay controls**

320

321 Colorimetric LAMP assays using the E1 primer set had relatively poor sensitivity and
322 slow amplification (Supplementary Fig. 1, 2A-C). In comparison assays duplexed with both E1
323 and N2 primer sets were more sensitive but resulted in relatively noisy luminance profiles
324 especially during the first five minutes of the reaction (Supplementary Fig. 2D-F). By
325 comparison assays with just the N2 primer set resulted in smooth luminance profiles and
326 detection of 5.25 ge/reaction in two out of three replicates (Fig. 1B-C). Luminance derivative
327 (L') profiles for positive standards amplified with N2 primer set had two identifiable peaks in
328 contrast to negative reactions which had relatively flat luminance profiles (Fig. 1D). We
329 subsequently chose to use the N2 primer set only in standardized reactions because of the robust
330 and clear luminance signals and sufficient performance to detect the vast majority of SARS-
331 CoV-2 positive samples based on reported saliva viral loads averaging 10^2 - 10^3 copies per
332 microliter.^{1,31}

333 Under optimized assay conditions the colorimetric luminance curve of PC standards is bi-
334 phasic with two distinct exponential growth phases in the first and last half of the reaction. We
335 quantitatively evaluated two curve features, presumably associated with initial amplification and
336 subsequent color change, at time intervals where a log-linear luminance profile was observed to
337 occur in PC assays. Specifically, local maxima in rates of luminance increase (L') occur between
338 5 and 20 minutes (L'_{MAX1}) and then again between 20 and 40 minutes (L'_{MAX2}) (Fig. 2A). The first

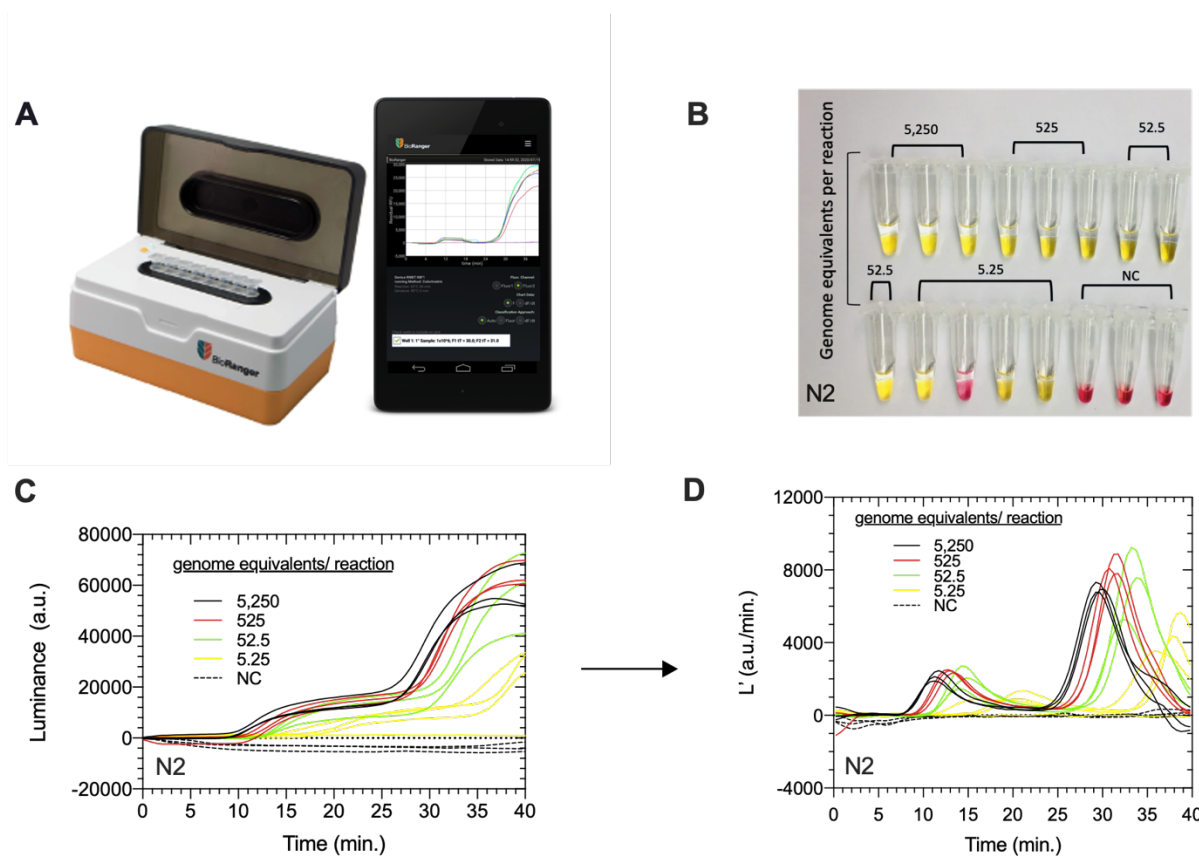
339 five minutes of luminance values were excluded from consideration for L'_{MAX1} because noise in
340 the baseline signal was previously observed to occur early in the reaction, particularly for assays
341 containing duplexed primer sets (Supplementary Fig. 2B, 2E).

342 The luminance curves of NC assays testing N2 primers (Fig. 1) plus five NC assays from
343 other trials conducted that day testing different primers sets (Supplementary Fig. 2) were pooled
344 (n=8) and compared to PC purified RNA standards (n=13, Fig. 1C-D). L'_{MAX2} was the only L' -
345 maxima that significantly ($P = 1.647e-006$) differentiated PC from NC based on differences
346 between means (PC - NC = 5,876 a.u./min., Fig. 2B, 2C). Correspondingly our decision
347 threshold for classifying positive control RNA standards was $L'_{MAX2} > 2764$ a.u./min., the
348 approximate equivalent to the pooled average of eight negative control assays ($\mu=394.4$
349 a.u./min.) plus 4.78 sample standard deviations ($sd=495.7$, $t_{.999}=4.78$, $dof=7$, $\alpha=0.001$). Using
350 this threshold, results from the colorimetric instrument are in 100% agreement with endpoint
351 visual assessment of yellow color, with both approaches detecting 3/4 assays containing 5.25
352 $\mu\text{g}/\text{reaction}$ with the N2 primer set, and every positive standard with more template RNA.

353 The times corresponding to the first luminance derivative peak (L'_{MAX1}) in the
354 colorimetric assay (10 – 20 minutes) were similar to threshold times observed in fluorescence-
355 based LAMP assays with the same primers (Fig. 2D). These results contrast sharply with
356 previous studies showing that incubation times of forty to fifty minutes are required for reliable
357 color development and end-point detection of SARS-CoV-2 colorimetric LAMP assays.^{12,29,32}
358 This indicates that our simple instrument is able to detect subtle changes in the optical
359 characteristics of the reaction that occur before easily observable color changes. The second
360 luminance derivative peaks (L'_{MAX2}) in our instrument are much larger than L'_{MAX1} and are
361 typically observed between 25-35 minutes into the reaction which is more consistent with times

362 required for endpoint assays, suggesting that this shift is primarily due to the spectral shift in the
363 pH indicator.

364



365

366

367 **Figure 1. Visual and quantitative results of colorimetric-LAMP assay controls. A)**

368 BioRanger diagnostic platform modified for colorimetric LAMP, interfaced to a smartphone app

369 that records luminance. B) Photograph of completed colorimetric LAMP assays performed under

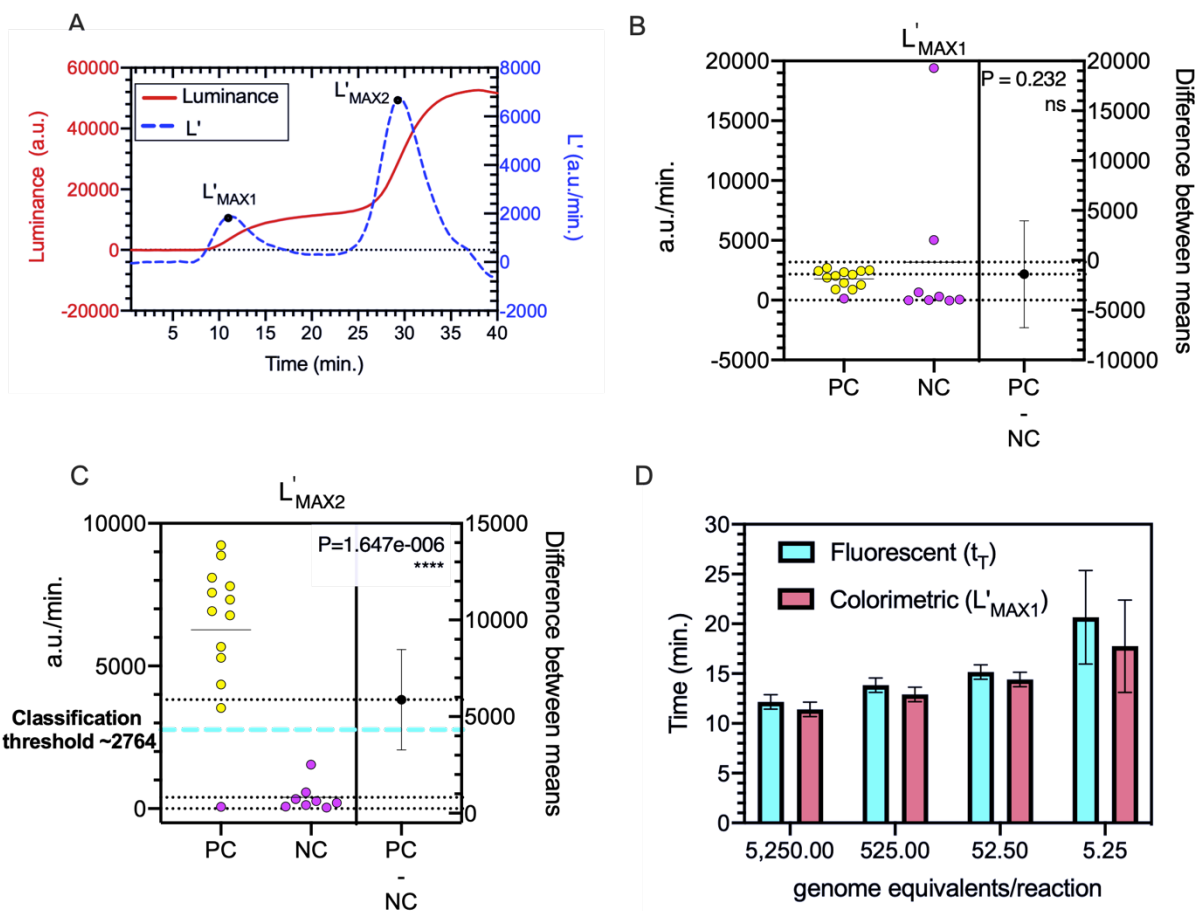
370 optimized reactions conditions for N-gene of synthetic SARS-CoV-2 RNA in water standards

371 and corresponding C) luminance (L) and D) luminance derivative (L') amplification curves as a

372 function of time for each standard replicate.

373

374



375

376

377 **Figure 2. Quantitative analysis of positive (PC) and negative control (NC) synthetic RNA**

378 **standards in water. A)** Example luminance (L) curve (left y-axis) and corresponding derivative

379 (L', right y-axis) of an optimized positive control assay containing 5,250 genome equivalents and

380 targeting the N-gene of synthetic SARS-CoV-2 RNA. The two derivative curve peaks indicate

381 local maxima in rate of change in luminance, measured in arbitrary units (a.u.) between 5-20

382 minutes (L'_{MAX1}) and between 20-40 minutes (L'_{MAX2}). **B)** Scatter plot of first (L'_{MAX1}) and **C)**

383 second (L'_{MAX2}) local maxima in luminance derivative (L') values (a.u./min.). PC (n=13) and NC

384 assays (n=8) were significantly (**** = P < 0.0005) different based on L'_{MAX2}. The N-gene was

385 quantitatively detected in 12/13 PC reactions containing a range of synthetic RNA (5.25 – 5,250
386 ge/reaction) in which $L'_{MAX2} > \sim 2764$ a.u./min. (classification threshold = blue dash line).
387 Symbols represent one assay replicate; color corresponds to endpoint reaction color and lines
388 represent the mean. The difference between PC and NC (PC-NC, right y-axis) contains three
389 values: the lower and upper 99% confidence level (dotted lines) and the difference between the
390 means of the two groups (error bars) **D**) Threshold values (t_T) corresponding to the time of
391 detection of the N-gene in PC LAMP assays performed in parallel on a commercial fluorescence-
392 enabled BioRanger correlated strongly to the time when L'_{MAX1} occurs. Error bars are standard
393 error of mean (SEM).

394

395 **Limit of detection in saliva**

396

397 The sensitivity of the colorimetric-LAMP assay was quantitatively assessed by following
398 optimized assay protocols for detection of SARS-CoV-2 in saliva using a handheld instrument
399 for luminance readout (Fig. 3). To reduce the impact of saliva-bound nuclease activity, we
400 supplemented the reaction buffer with Tris-EDTA (TE) to stabilize the viral genomic RNA
401 released from the capsid following heat treatment of viral samples. EDTA protects nucleic acids
402 from degradation by chelating the nuclease cofactor Mg^{2+} and Tris maintains a pH above 7.5, at
403 which nucleases are less active. Researchers at the University of Illinois extensively evaluated
404 cheaper alternatives to commercial sample transport buffers containing expensive and
405 proprietary viral RNA-stabilizing agents like DNA/RNA Shield (Zymo Research), and
406 demonstrated that TE buffer is effective at stabilizing nucleic acids for sensitive detection (500-
407 1000 viral particles per mL) by RT-qPCR.²⁰ We similarly demonstrated that addition of TE to

408 heat-inactivated samples containing intact gamma-irradiated SARS-CoV-2 improved the LOD of
409 the colorimetric assay by an order of magnitude compared to spiked samples diluted in water
410 only (Supplementary Fig. 3). Furthermore, their research suggests that extended heating of the
411 sample (i.e. 30 minutes, 95°C) inactivates inhibitors in saliva whereas standard protocols for heat
412 inactivation of SARS-CoV-2 at lower temperatures (i.e. 30 minutes, 60°C) did not allow for
413 sensitive detection. Herein spiked saliva samples are subjected to heat treatments at 95°C for 30
414 min prior to diluting the sample 1:1 with TE buffer.

415 Reactive controls (RC) containing inactivated SARS-CoV-2 in saliva were classified as
416 positive for detection if L'_{MAX2} was greater than 660 a.u./min, equivalent to the approximate
417 average ($\mu=86.09$ a.u./min.) plus 4.78 standard deviations ($sd=119.1$, $t_{.999}=4.78$, $dof=7$, $\alpha=0.001$)
418 of eight non-reactive control (NRC) (Fig. 4A). Applying this classification threshold, the
419 luminance-based LOD, defined by the lowest concentration where SARS-CoV-2 is detected in
420 all replicates, is 5×10^4 ge/mL corresponding to 50 ge/reaction (Fig. 4B). Luminance
421 amplification curves for this section can be found in Supplementary Figure 4.

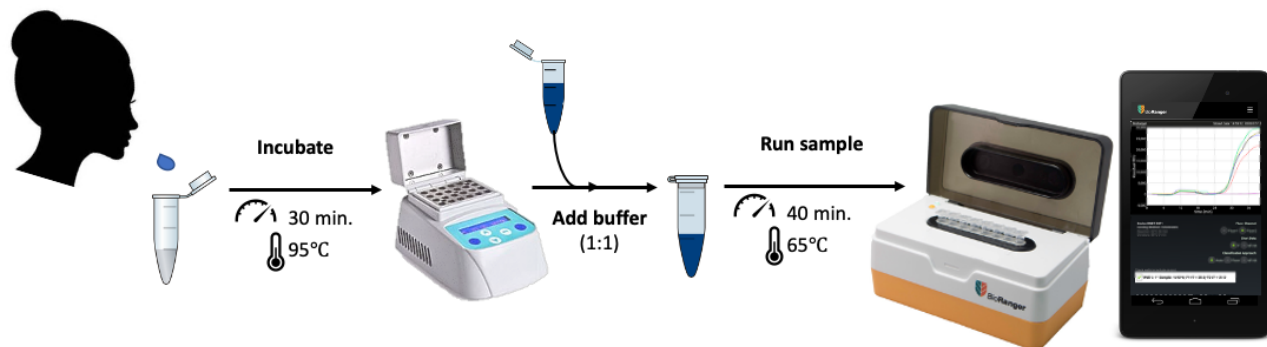
422 SARS-CoV-2 was detected both visually and quantitatively below the LOD (5×10^3 ge/mL –
423 2.5×10^4 ge/mL) in some replicates but at a lower rate. In some reactive samples below the LOD
424 and in reactions in which SARS-CoV-2 was not visually detected, a low-amplitude luminance
425 signal ($L'_{MAX2} < 1,000$ a.u./min) is observed in the last twenty minutes. This could indicate latent
426 target amplification and a longer reaction time could improve sensitivity of small quantities of
427 viral RNA. However longer incubation times (> 40 minutes) have shown to increase the false
428 positive rate. One NRC reaction showed a color change, however the L'_{MAX2} values were less
429 than 100 a.u./min. The yellow/orange NRC reaction was quantitatively classified as ‘Not
430 Detected’ reducing the initial false positive (FP) rate of visual end-point determination from

431 12.5% (1/8 NRC turned orange/yellow) to 0%. The color change in the negative control may
432 have occurred from the saliva destabilizing the buffer system demonstrating the importance of
433 quantitative approaches to reduce the prevalence of false positives.

434

435

436



437

438

439 **Figure 3. Schematic representation of colorimetric LAMP workflow to quantitatively**

440 **detect SARS-CoV-2 in saliva using a handheld isothermal diagnostic platform.** The

441 optimized saliva testing protocol is as follows: 1-2 mL of saliva is collected, heat inactivated (95

442 °C for 30 minutes) then combined with equal parts TE buffer (1X, 1% Tween 20). Next 2 μ L of

443 the diluted saliva sample is directly pipetted into a reaction tube containing Mastermix and

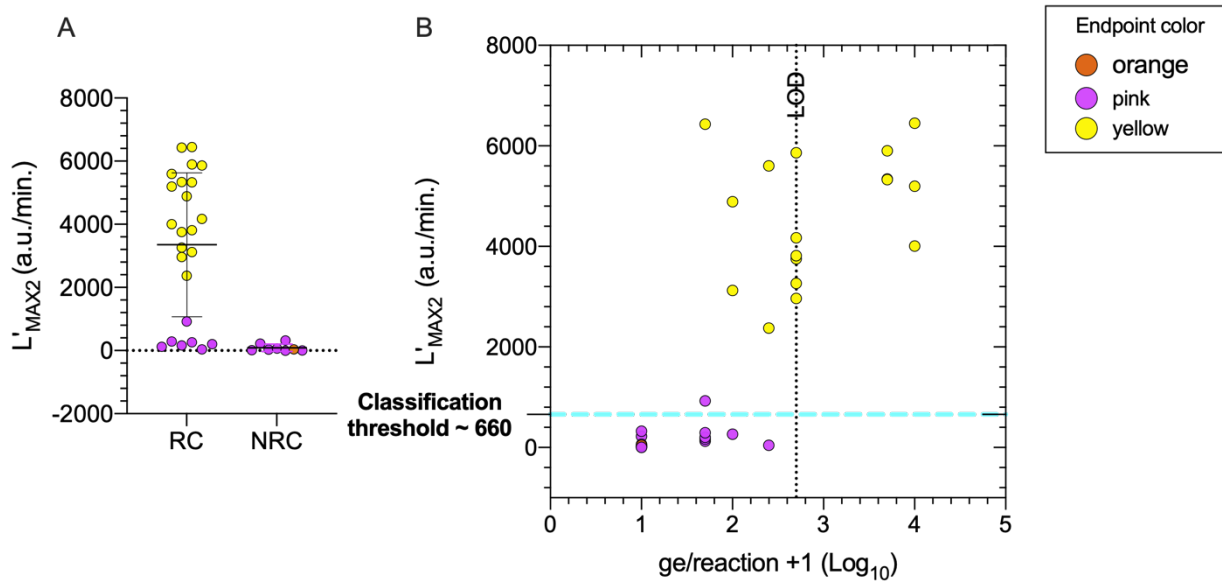
444 primers and incubated (65 °C for 40 minutes) on the BioRanger: a mobile isothermal diagnostic

445 platform capable of performing eight assays in parallel. Real-time luminance data is recorded on

446 a custom smartphone app for post-test analysis of the results.

447

448



449

450 **Figure 4. Quantitative and visual detection sensitivity of inactivated SARS-CoV-2 in**

451 **saliva. A)** Comparison of maximum amplification rates (L'_{MAX2}) between reactive controls (RC)

452 containing viral RNA and non-reactive control (NRC) saliva samples. Error bars represent mean

453 and standard deviation. **B)** The LOD (dotted line; lowest concentration where the N-gene is

454 detected in all replicates) by endpoint and luminance-based detection ($L'_{MAX2} > 660$ a.u./min.) is

455 50 ge/reaction equivalent to 5×10^4 ge/mL in the primary sample. The color of each symbol,

456 representing an assay replicate, corresponds to the endpoint color of the assay.

457

458

459 **Blind evaluation of the colorimetric LAMP assay using clinically contrived**

460 **saliva samples**

461

462 To evaluate the feasibility and performance of our quantitative colorimetric LAMP

463 method, a blinded and randomized contrived clinical trial was conducted. A total of 20 saliva

464 samples, 10 reactive controls containing inactivated SARS-CoV-2 at 1X and 2X the LOD (5 x
465 10^4 ge/mL) determined from saliva standards (Fig. 4), and 10 non-reactive controls (0 ge/mL),
466 were tested using the standardized protocol (Fig. 3). In addition to two replicate assays for the N-
467 gene, each sample was subjected to a test panel including two replicates each of an internal
468 control reaction (IC; for human β -actin), a positive control (PC; supplemented with 10^6
469 ge/reaction synthetic RNA), and a negative control with no sample or supplemental RNA. Each
470 individual assay of the test panel was interpreted both visually (pink = Not detected,
471 yellow/orange = Detected) as well as quantitatively, using the previously established luminance
472 readout classification threshold determined from saliva standards ($L'_{MAX2} > 660$ a.u./min =
473 Detected, $L'_{MAX2} < 660$ a.u./min. = Not detected). A test panel was interpreted as 'Detect' if
474 SARS-CoV-2 N-gene was detected in 2/2 replicates, 'Detected†' for 1/2 replicates and 'Non-
475 detect' for 0/2 replicates. Additionally, the panel results were deemed valid if both replicates for IC
476 (2/2) and PC (2/2) were detected and neither NC (0/2) replicates were detected. Panels with any
477 unexpected outcome of control reactions is classified as 'Inconclusive'. Examples of three test
478 panels are shown in Figure 5; detailed results for all 20 diagnostic panels are included in
479 Supplementary Figure 5, and the sample pairing key is shown in Supplementary Table 2.

480 Although the test panels were run on two colorimetry-enabled BioRanger instruments
481 over two weeks and by multiple experimenters using different batches of reagent stocks,
482 performance analysis demonstrates that the method sensitivities, specificities and accuracy to
483 quantitatively detect SARS-CoV-2 did not vary substantially. All assays that resulted in an
484 endpoint color of yellow also showed luminance signal amplification rate above decision
485 threshold values where L'_{MAX2} was above 660 a.u./min. (Fig. 6A). A failed color change at the
486 LOD correlated with no or low intensity luminance signals ($L'_{MAX2} < 660$). The SARS-CoV-2 N-

487 gene was detected in all test sample replicates (10/10) for saliva samples spiked with 1×10^5
488 ge/mL (2X LOD). At least one replicate tested positive for each sample with 5×10^4 ge/mL (1X
489 LOD), though not all replicates at this concentration tested positive (6/10) (Fig. 6B). SARS-
490 CoV-2 was not detected in any of the contrived negative samples (NRC). Human ACTB gene
491 was detected in all but one test panel IC (19/20 samples, 38/40 replicates).

492 Sample 1 and sample 2 (Supplementary Fig. 5) were the first panels run on the day of
493 testing and performed in parallel on two different instruments without first pre-heating the
494 incubation chamber. This resulted in significant amount of noise in all assays of Panel 1 and one
495 NRC assay of Panel 2. Panel 2 NRC assay was noisy from 0-25 minutes, resulting in an L'_{MAX2}
496 value of 746 a.u./min. However, after inspection of the smoothed and corrected L' curve, it was
497 clear that the local maxima (L'_{MAX2}) was an artifact due to noise and the assay was classified as
498 'Not-detected'. Subsequently all tests were performed on pre-heated incubation blocks reaching
499 a temperature of at least 50 °C prior to loading the reaction tubes. This phenomenon was
500 observed in preliminary experiments but not well characterized and in most cases, the luminance
501 curve corrections and smoothing were sufficient to remove noise or artifacts falsely indicating
502 amplification.

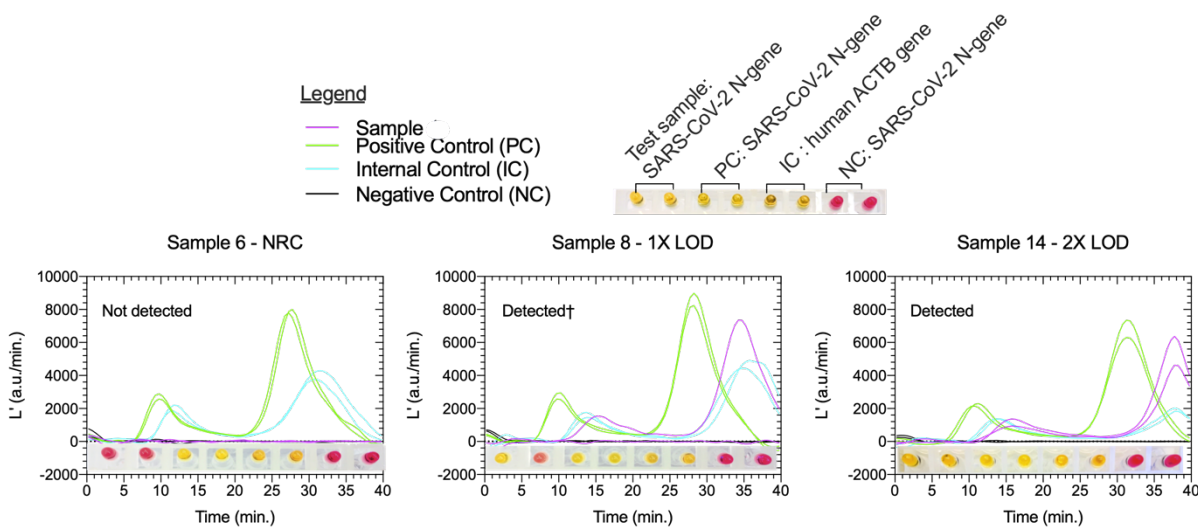
503 Panel 9 tested an NRC sample, and even though endpoint assessment of the color (light
504 orange) resulted in positive classification for both replicates, no signs of amplification were
505 observed in the luminance data. Using the real-time data, both classified correctly as negative
506 (Supplementary Fig. 5, panel 9). Similarly, one replicate of the panel 3 sample (also an NRC
507 sample) was light orange incorrectly indicating amplification based on endpoint color, though
508 the luminance data correctly showed no amplification (Supplementary Fig. 5, panel 3). In
509 contrast the internal control reactions on panel 9 showed evidence of faint and late amplification

510 in the luminance data but failed to meet threshold for positive classification, resulting in this
511 panel being inconclusive, even though the endpoint color of these internal controls was yellow
512 (positive). The N-gene was correctly detected in all positive control replicates (40/40) and not
513 detected in any of the negative control replicates (0/40) (Fig. 6A-B).

514 The L'_{MAX2} values provide a robust indication of nucleic acid amplification that may not
515 accompany an endpoint color change that is sensitive to variations in sample characteristics. This
516 suggests that dynamically monitoring luminescence might improve classification accuracy where
517 sample pH is too low, in addition to situations in which buffering capacity is too high to yield a
518 complete red to yellow color change. In comparison, classification based on endpoint color in
519 our panels results in a false positive rate of 10% near the LOD.

520

521



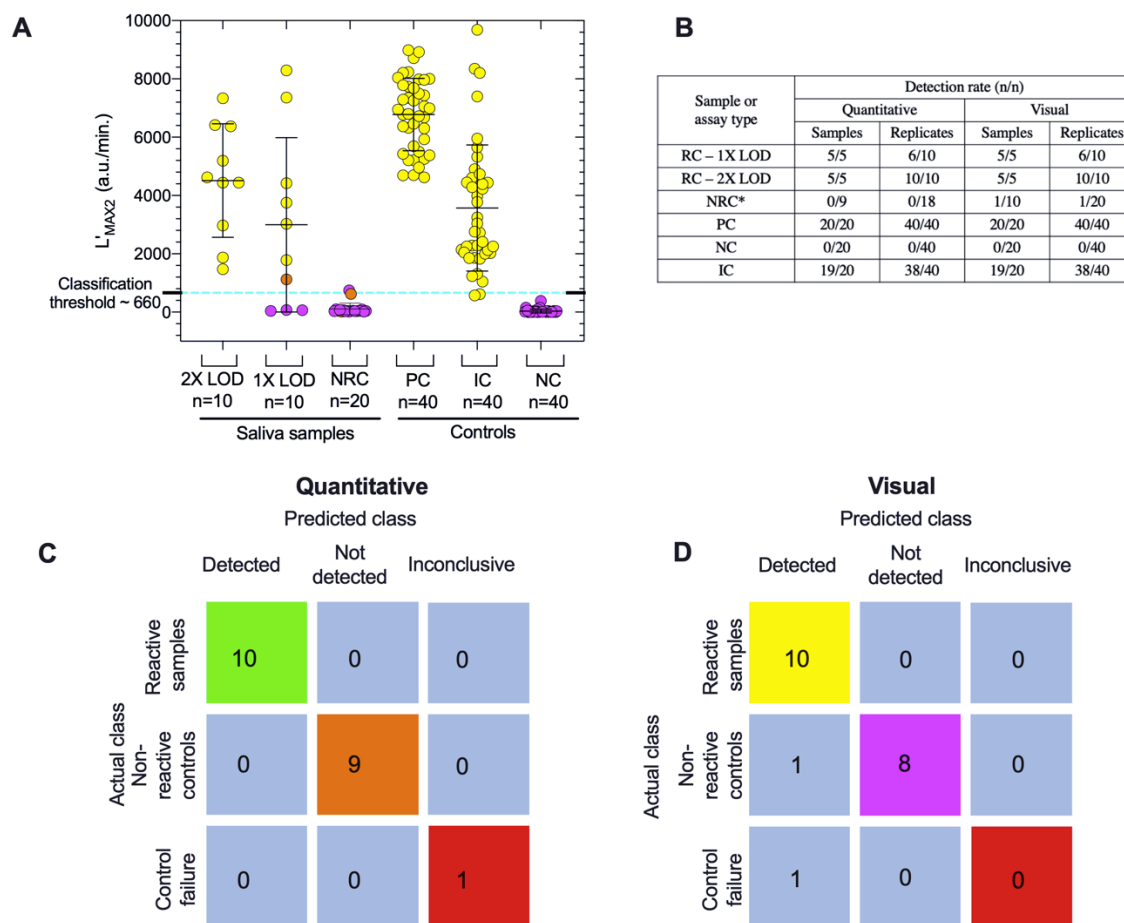
522

523

524 **Figure 5. Example test panel configuration and results for each three sample types**

525 **evaluated in the contrived clinical testing trial.** Test panel results are interpreted both visually

526 (pink = target not detected, yellow = target detected) and by luminance derivatives (L'). The test
 527 panels are interpreted based on the detection rate of SARS-CoV-2 N-gene in tested saliva
 528 samples as : 'Not detected' (0/2), 'Detected†' (1/2) or 'Detected' (2/2) if PC and IC assay targets
 529 are detected in all replicates and not detected in any NC replicates. In these three panels shown,
 530 visual and quantitative results are in 100% agreement for all assays. The results of all 20 saliva
 531 test panels can be found in Supplementary Figure 5.
 532



533
 534 **Figure 6. Performance analysis comparison of the quantitative colorimetric LAMP assay to**
 535 **visual detection using twenty clinical SARS-CoV-2 saliva test panels. (A) Distribution**

536 summary of L'_{MAX2} values for each tested saliva sample and control group used in the clinical
537 evaluation trial. Blue dotted line represents classification threshold value ($L'_{MAX2} > 660$ a.u./min.)
538 used to quantitatively determine whether the assay target is positively detected. Group means are
539 indicated by lines, error bars are the standard deviation and the symbol color corresponds to the
540 endpoint reaction color (orange, pink, yellow). **(B)** Table comparing visual to quantitative
541 sensitivity in terms of sample and replicate detection rates for every sample and control group.
542 *NRC sample sizes are different due to IC failure only recognized by quantitative analysis of
543 panel 9 **(C, D)** Confusion tables comparing quantitative and visual test panel interpretations
544 (SARS-CoV-2 Detected, Not Detected or Inconclusive) made blindly by the experimenter to the
545 actual classification of tested samples.

546

547

548 **Discussion**

549

550 As COVID-19 continues to surge, there is increasing need to expand points-of-care and
551 mobile testing platforms to quell the transmission of this virus. Nucleic acid amplification
552 emerged as the gold standard for detection efficiency in the early months of the pandemic
553 because this method is both highly specific and highly sensitive. Paired with an RNA isolation
554 sample-processing step, RT-PCR-based SARS-CoV-2 detection assays provided the necessary
555 data for viral transmission rates and initial contact tracing. RT-PCR-based testing, while accurate
556 and sensitive, is heavily reliant on thermocycling equipment that requires a specialized
557 laboratory environment and highly trained personnel to operate. These limitations have hindered
558 effort to scale the use of this testing platform to meet the exponential expansion in testing

559 demand. Antibody-based detection platforms are emerging as an alternative to RT-PCR based
560 assays to meet the rising demand for rapid, point-of-care testing. While antibody-based detection
561 methods can be adapted for at-home, point-of-care detection, or mobile testing, this methodology
562 is inherently less sensitive than nucleic acid amplification-based assays.

563 Isothermal nucleic acid amplification merges the mobility of antibody-based assays with
564 the high sensitivity of RT-PCR as an efficient platform to expand COVID-19 testing. In this
565 study, we have built upon the colorimetric endpoint readout of LAMP-based testing and have
566 provided proof-of-design for a mobile platform that utilizes isothermal nucleic acid amplification
567 in conjunction with direct detection of SARS-Cov-2 from saliva. We have paired SARS-CoV-2
568 detection during isothermal nucleic acid amplification with a mobile, handheld device that
569 detects colorimetric changes during isothermal amplification similar to that of a microplate
570 reader used in previous studies.¹² This method is capable of detecting purified (synthetic) SARS-
571 CoV-2 RNA template within an order of magnitude of single particle detection (5.25
572 genomes/reaction) therefore comparable to the theoretical maximum sensitivity of other RT-
573 PCR-based approaches as well as other LAMP-based SARS-CoV-2 detection designs.

574 COLOR initially received FDA approval for merging LAMP-based testing with a
575 colorimetric endpoint readout that streamlined detection and circumvented the need for highly
576 specialized diagnostic equipment. The majority of FDA-approved LAMP-based assays have only
577 been authorized for samples that have first undergone RNA purification. In order to develop a
578 direct-detection assay from saliva samples that can vary in pH, nucleic acid amplification and pH
579 change must be measured independently. Previous studies have examined the accuracy and
580 sensitivity of endpoint colorimetric changes indirectly by conducting parallel experiments with
581 real-time fluorescent-based assays.^{13,33,34} These approaches, however, cannot directly verify

582 whether a colorimetric readout corresponds to amplification or a spurious pH change. This
583 indirect approach has hindered progress towards developing a direct-detection assay from saliva
584 samples. Our approach, however, provides a platform to independently measure both nucleic
585 acid amplification and colorimetric endpoint readout for every sample and provide a means to
586 determine whether SARS-CoV-2 can be detected directly from saliva.

587 Using a commercial BioRanger, the time course of the initial luminance derivative peak,
588 L'_{MAX1} , corresponded to the time to the threshold of detection for fluorescent-based LAMP
589 assays, while the time course of the second luminance derivative peak, L'_{MAX2} , corresponded to
590 the times reported to be required for endpoint color change. These data indicate that our method
591 can detect subtle optical changes at the initiation of LAMP amplification, perhaps due to
592 increased scattering from small particulates of magnesium pyrophosphate, as well as more
593 intense optical changes later in the reaction corresponding to transition of pH through the pK_a of
594 the phenol red indicator. The modified BioRanger, therefore, provides an ideal platform for
595 evaluating whether a LAMP-based assay can be implemented for the direct detection of SARS-
596 Cov-2 from saliva.

597 Direct detection of viral particles from saliva can present a host of additional
598 complications. In addition to fluctuations in pH that can destabilize the viral capsid or cause a
599 spurious color change, saliva contains nucleases that can degrade the viral genome, reducing the
600 amount of virus that can be detected by LAMP. Previous work has shown that encapsulated
601 SARS-CoV-2 is stable in saliva^{20,35,36} and isothermal nucleic acid amplification efficiency is
602 enhanced when the heat-inactivated saliva matrix is buffered with TE and Tween 20. Processing
603 samples in this way, we implemented a low-cost alternative to VTM that was completely

604 compatible with both luminance detection and endpoint colorimetric detection of isothermal
605 amplification of SARS-Cov-2 nucleic acid.

606

607 *Future Implementation*

608 Through the assay that we developed in this study, we were able to directly detect
609 inactivated SARS-CoV-2 from saliva with an LOD of 50 genomes/reaction. This detection
610 sensitivity is similar to a previously-described LAMP-based SARS-CoV-2 direct detection assay
611 used in conjunction with nasopharygeal samples stabilized in VTM.³⁷ In October of 2020,
612 COLOR's rapid LAMP test was deployed at the San Francisco International airport for onsite
613 passenger testing as one of the "Trusted Testing and Travel Partners" in Hawaii's pre-travel
614 COVID-19 testing program developed to encourage safe travel, tourism and re-opening of the
615 economy. The methods presented here can be adapted in a similar way to provide real-time
616 monitoring as a companion diagnostic to colorimetric endpoint detection of SARS-CoV-2
617 amplification from easy-to-collect saliva samples. This approach has the potential to reduce the
618 cost and invasive nature of COVID-19 testing and can be broadly applied to point of care
619 detection in field surveillance programs or in remote clinical settings.

620

621

622

623

624

625

626

627

628 **Acknowledgements**

629 We would like to thank Dr. John M. Berestecky (Professor, Microbiology and
630 Biotechnology, Kapiolani Community College, Honolulu, HI; Director of the Monoclonal
631 Antibody Service Facility and Training Program) and Dr. Rebecca Kanenaka, (State Certified
632 Microbiologist and CLIA Certified Lab Director, Kapiolani Community College Honolulu, HI)
633 for their roles as project advisors, community outreach and assistance with IBC protocol
634 certification and experimental design, as well as Dr. Reinhold Penner and Dr. Andrea Fleig for
635 reagents and equipment. This project could not have been completed without the generous
636 donation of colorimetric assay reagents from Nathan Tanner (New England Biolabs) who early
637 on during the pandemic also shared LAMP primer sequences used in this study. This research is
638 part of a global initiative, referred to as ‘gLAMP’, to validate LAMP diagnostics for the
639 detection SARS-CoV-2 and we thank all participating members who helped guide our testing
640 protocols from labs across the world. Finally, we express our gratitude to Diagenetix Inc.
641 (Honolulu, HI) for use and deconstruction of commercial BioRanger units and for continued
642 technical support.

643

644

645

646

647

648

649

650

651

652 **References**

- 653 1. Wyllie AL, Fournier J, Casanovas-Massana A, et al. Saliva is more sensitive for SARS-
654 CoV-2 detection in COVID-19 patients than nasopharyngeal swabs. *medRxiv*.
655 2020;(2):2020.04.16.20067835. doi:10.1101/2020.04.16.20067835
- 656 2. Vaz SN, Santana DS de, Netto EM, et al. Saliva is a reliable, non-invasive specimen for
657 SARS-CoV-2 detection. *Brazillian J Infect Dis*. 2020;24(5):422-427.
- 658 3. Altawalah H, Alhuraish F, Ali W, Ezzikouri S. Saliva specimens for detection of severe
659 acute respiratory syndrome coronavirus 2 in Kuwait: A cross-sectional study.
660 2020;(January).
- 661 4. Keremane ML, Ramadugu C, Rodriguez E, et al. A rapid field detection system for citrus
662 huanglongbing associated “*Candidatus Liberibacter asiaticus*” from the psyllid vector,
663 *Diaphorina citri* Kuwayama and its implications in disease management. *Crop Prot*.
664 2015;68:41-48. doi:10.1016/j.cropro.2014.10.026
- 665 5. Kubota R, LaBarre P, Singleton J, et al. Non-instrumented nucleic acid amplification
666 (NINA) for rapid detection of *Ralstonia solanacearum* race 3 biovar 2. *Biol Eng Trans*.
667 2011;4(2):69-80. doi:10.13031/2013.38508
- 668 6. Larrea-Sarmiento A, Dhakal U, Boluk G, et al. Development of a genome-informed loop-
669 mediated isothermal amplification assay for rapid and specific detection of *Xanthomonas*
670 *euvesicatoria*. *Sci Rep*. 2018;8(1):1-11. doi:10.1038/s41598-018-32295-4
- 671 7. Color. SARS-CoV-2 RT-LAMP Diagnostic Assay. <https://www.color.com/wp->

- 672 content/uploads/2020/10/Color-LAMP-Diagnostic-Assay_v2_Updated-101420_3.pdf.
673 Published 2020. Accessed December 20, 2020.
- 674 8. Yamamoto N, Hamaguchi S, Akeda Y, et al. Clinical specimen-Direct LAMP: A useful
675 tool for the surveillance of blaOXA-23-Positive carbapenem-resistant *acinetobacter*
676 *baumannii*. *PLoS One*. 2015;10(7):1-10. doi:10.1371/journal.pone.0133204
- 677 9. Francois P, Tangomo M, Hibbs J, et al. Robustness of a loop-mediated isothermal
678 amplification reaction for diagnostic applications. *FEMS Immunol Med Microbiol*.
679 2011;62(1):41-48. doi:10.1111/j.1574-695X.2011.00785.x
- 680 10. Howson ELA, Kurosaki Y, Yasuda J, et al. Defining the relative performance of
681 isothermal assays that can be used for rapid and sensitive detection of foot-and-mouth
682 disease virus. *J Virol Methods*. 2017;249(August):102-110.
683 doi:10.1016/j.jviromet.2017.08.013
- 684 11. Genome Web. Coronavirus Test Tracker: Commercially Available COVID-19 Diagnostic
685 Tests. 360 Dx. <https://www.360dx.com/coronavirus-test-tracker-launched-covid-19-tests>.
686 Published 2020. Accessed December 20, 2020.
- 687 12. The FOR, Genomics C, Diagnostic S-L. Color Genomics SARS-CoV-2 LAMP Diagnostic
688 Assay EUA Summary. 2020:1-13.
- 689 13. Tanner NA, Zhang Y, Evans TC. Visual detection of isothermal nucleic acid amplification
690 using pH-sensitive dyes. *Biotechniques*. 2015;58(2):59-68. doi:10.2144/000114253
- 691 14. Abbott. Id now TM product insert.
- 692 15. Moghbelli H, Ellithy K, Eslami Z, et al. Performance of Abbott ID NOW rapid SARS-
693 CoV-2 NAAT. *Block Caving – A Viable Altern*. 2020;21(1):1-9.
694 doi:10.1016/j.solener.2019.02.027

- 695 16. Vashist SK. In vitro diagnostic assays for COVID-19: Recent advances and emerging
696 trends. *Diagnostics*. 2020;10(4). doi:10.3390/diagnostics10040202
- 697 17. Griesemer S, Van Slyke G, Ehrbar D, et al. Evaluation of specimen types and saliva
698 stabilization solutions for SARS-CoV-2 testing. 2020;701:1-34.
699 doi:10.1101/2020.06.16.20133041
- 700 18. Anahtar M, McGrath GE, Rabe B, et al. Clinical assessment and validation of a rapid and
701 sensitive SARS-CoV-2 test using reverse-transcription loop-mediated isothermal
702 amplification. 2020:1-22. doi:10.1101/2020.05.12.20095638
- 703 19. Gray AN, Ph D, Ren G, et al. Facilitating Detection of SARS-CoV-2 Directly from Patient
704 Samples : Precursor Studies with RT-qPCR and Colorimetric RT-LAMP Reagents. *New*
705 *Engl Biolabs*. 2020:1-5.
- 706 20. Ranoa DRE, Holland RL, Alnaji FG, et al. Saliva-Based Molecular Testing for SARS-
707 CoV-2 that Bypasses RNA Extraction. *bioRxiv*. 2020:2020.06.18.159434.
708 doi:10.1101/2020.06.18.159434
- 709 21. Kariwa H, Fujii N, Takashima I. Inactivation of SARS coronavirus by means of povidone-
710 iodine, physical conditions and chemical reagents. *Dermatology*. 2006;212(SUPPL.
711 1):119-123. doi:10.1159/000089211
- 712 22. Anahtar MN, McGrath GEG, Rabe BA, et al. Clinical assessment and validation of a rapid
713 and sensitive SARS-CoV-2 test using reverse-transcription loop-mediated isothermal
714 amplification. *Medrxiv*. 2020:1-22. doi:10.1101/2020.05.12.20095638
- 715 23. Fomsgaard AS, Rosenstjerne MW. An alternative workflow for molecular detection of
716 SARS-CoV-2 - Escape from the NA extraction kit-shortage, Copenhagen, Denmark,
717 March 2020. *Eurosurveillance*. 2020;25(14):1-8. doi:10.2807/1560-

- 718 7917.ES.2020.25.14.2000398
- 719 24. Zhang Y, Ren G, Buss J, Barry AJ, Patton GC, Tanner NA. Enhancing colorimetric loop-
720 mediated isothermal amplification speed and sensitivity with guanidine chloride.
721 *Biotechniques*. 2020. doi:10.2144/btn-2020-0078
- 722 25. New England Biolabs. WarmStart Colorimetric LAMP 2X Master Mix Typical LAMP
723 Protocol (M1800). [https://www.neb.com/protocols/2016/08/15/warmstart-colorimetric-](https://www.neb.com/protocols/2016/08/15/warmstart-colorimetric-lamp-2x-master-mix-typical-lamp-protocol-m1800)
724 [lamp-2x-master-mix-typical-lamp-protocol-m1800](https://www.neb.com/protocols/2016/08/15/warmstart-colorimetric-lamp-2x-master-mix-typical-lamp-protocol-m1800). Accessed September 1, 2020.
- 725 26. Kubota R, Jenkins DM. Real-Time duplex applications of Loop-Mediated AMPlification (
726 LAMP) by assimilating probes. *Int J Mol Sci*. 2015;(16):4786-4799.
727 doi:10.3390/ijms16034786
- 728 27. Kubota R, Alvarez AM, Su WW, Jenkins DM. FRET-Based Assimilating Probe for
729 Sequence-Specific Real-Time Monitoring of Loop-Mediated Isothermal Amplification
730 (LAMP). *Biol Eng Trans*. 2011;4(2):81-100.
- 731 28. Mitchell SL, St George K, Rhoads DD, et al. Understanding, verifying and implementing
732 Emergency Use Authorization molecular diagnostics for the detection of SARS-CoV-2
733 RNA. *J Clin Microbiol*. 2020;(May). doi:10.1128/JCM.00796-20
- 734 29. Gonzalez-Gonzalez E, Lara-Mayorga IM, Yee-de Leon F, et al. Scaling diagnostics in
735 times of COVID-19: Colorimetric Loop-mediated Isothermal Amplification (LAMP)
736 assisted by a 3D-printed incubator for cost-effective and scalable detection of SARS-CoV-
737 2. *medRxiv*. 2020:2020.04.09.20058651. doi:10.1101/2020.04.09.20058651
- 738 30. Lalli MA, Chen X, Langmade SJ, et al. Rapid and extraction-free detection of SARS-
739 CoV-2 from saliva with colorimetric LAMP. 2020.
- 740 31. To KKW, Tsang OTY, Leung WS, et al. Temporal profiles of viral load in posterior

- 741 oropharyngeal saliva samples and serum antibody responses during infection by SARS-
742 CoV-2: an observational cohort study. *Lancet Infect Dis.* 2020;20(5):565-574.
743 doi:10.1016/S1473-3099(20)30196-1
- 744 32. Kellner MJ, Ross JJ, Schnabl J, et al. A rapid, highly sensitive and open-access SARS-
745 CoV-2 detection assay for laboratory and home testing. *bioRxiv.* 2020:2020.06.23.166397.
746 doi:10.1101/2020.06.23.166397
- 747 33. Park GS, Ku K, Baek SH, et al. Development of Reverse Transcription Loop-mediated
748 Isothermal Amplification (RT-LAMP) Assays Targeting SARS-CoV-2. *J Mol Diagn.*
749 2020;(May):1-8. doi:10.1016/j.jmoldx.2020.03.006
- 750 34. Kellner M, Ross J, Schnabl J, et al. A rapid, highly sensitive and open-access SARS-CoV-
751 2 detection assay for laboratory and home testing. 2020:1-28.
752 doi:10.1101/2020.06.23.166397
- 753 35. Simonov M, Datta R, Handoko R, et al. Saliva or Nasopharyngeal Swab Specimens for
754 Detection of SARS-CoV-2. *N Engl J Med.* 2020;383:1283.
- 755 36. Ceron J, Lamy E, Martinez-Subiela S, et al. Use of Saliva for Diagnosis and Monitoring
756 the SARS-CoV-2: A General Perspective. *J Clin Med.* 2020;9(5):1491.
757 doi:10.3390/jcm9051491
- 758 37. Ganguli A, Mostafa A, Berger J, et al. Rapid isothermal amplification and portable
759 detection system for SARS-CoV-2. *Proc Natl Acad Sci U S A.* 2020;117(37):22727-
760 22735. doi:10.1073/pnas.2014739117
- 761